HHS Public Access

Author manuscript

Cell Microbiol. Author manuscript; available in PMC 2020 March 01.

Published in final edited form as:

Cell Microbiol. 2019 March ; 21(3): e12967. doi:10.1111/cmi.12967.

Aggregatibacter actinomycetemcomitans leukotoxin causes activation of lymphocyte function-associated antigen 1

Patrik Nygren[1,3,*], **Nataliya Balashova**[2], **Angela C. Brown**[2,†], **Irene Kieba**[2,‡], **Anuradha Dhingra**[1], **Kathleen Boesze-Battaglia**[1], **Edward T. Lally**[2]

[1]Departments of Biochemistry, University of Pennsylvania, Philadelphia, Pennsylvania

[2]Departments of Pathology, School of Dental Medicine, and the Division of Hematology/Oncology, University of Pennsylvania, Philadelphia, Pennsylvania

[3]Department of Medicine, School of Medicine, University of Pennsylvania, Philadelphia, Pennsylvania

Abstract

Repeats-in-toxin leukotoxin (LtxA) produced by the oral bacterium *Aggregatibacter actinomycetemcomitans* kills human leukocytes in a lymphocyte function-associated antigen 1 (LFA-1, integrin α_L/β_2)-dependent manner, although the mechanism for this interaction has not been identified. The LtxA internalisation by LFA-1-expressing cells was explored with florescence resonance energy transfer (FRET) microscopy using a cell line that expresses LFA-1 with a cyan fluorescent protein-tagged cytosolic α_L domain and a yellow fluorescent protein-tagged β_2 domain. Phorbol 12-myristate 13-acetate activation of LFA-1 caused transient cytosolic domain separation. However, addition of LtxA resulted in an increase in FRET, indicating that LtxA brings the cytosolic domains closer together, compared with the inactive state. Unlike activation, this effect was not transient, lasting more than 30 min. Equilibrium constants of LtxA binding to the cytoplasmic domains of both α_L and β_2 were determined using surface plasmon resonance. LtxA has a strong affinity for the cytosolic domains of both the α_L and β_2 subunits (K_d = 15 and 4.2 nM, respectively) and a significantly lower affinity for the cytoplasmic domains of other integrin α_M, α_X, and β_3 subunits (K_d = 400, 180, and 230 nM, respectively), used as controls. Peptide fragments of α_L and β_2 show that LtxA binds membrane-proximal domain of α_L and intermediate domain of β_2.

Keywords

integrin; leukotoxin (LtxA); LFA-1; microbial pathogenesis; RTX toxin; surface plasmon resonance (SPR)

Correspondence Edward T. Lally, DMD, PhD, Department of Pathology, School of Dental Medicine, and the Division of Hematology/Oncology, University of Pennsylvania, 240 S. 40th St., 317 Levy Building, Philadelphia, PA 19104., lally@upenn.edu.

*__Present Address__ Bioarctic AB, SE-11251 Stockholm, Sweden

†Department of Chemical Engineering Lehigh University Bethlehem, PA 18015

‡Deceased

SUPPORTING INFORMATION

Additional supporting information may be found online in the Supporting Information section at the end of the article.

1 | INTRODUCTION

Aggregatibacter actinomycetemcomitans (*Aa*), a facultative anaerobic bacterium of the *Pasteurellaceae* family, is commonly found in the upper aerodigestive tract of man and certain higher primates (Taichman et al., 1987). *Aa* is the etiologic agent of localised aggressive (juvenile) periodontitis (LAP), an aggressive form of periodontal disease in adolescents. The organism produces a 114 kDa repeats in toxin (RTX; Welch, 1991) or leukotoxin (LtxA) that primarily expresses a specificity for human and primate immune cells (Baehni et al., 1981; Baehni, Tsai, McArthur, Hammond, & Taichman, 1979; Kachlany et al., 2010; Tsai, McArthur, Baehni, Hammond, & Taichman, 1979). Leukocytes from rodent species can be affected by higher concentrations of LtxA (DiFranco, Kaswala, Patel, Kasinathan, & Kachlany, 2013). A number of studies suggested the pivot role of LtxA in LAP development. *Aa* isolated from LAP patients was found to belong to a single serotype b strain JP2 (Haubek & Johansson, 2014; Shahabuddin, Boesze-Battaglia, & Lally, 2016), which is characterised by increased LtxA production (Brogan, Lally, Poulsen, Kilian, & Demuth, 1994). There is evidence for the link between leukotoxicity and the periodontal attachment loss (Hoglund Aberg, Haubek, Kwamin, Johansson, & Claesson, 2014). LtxA may help the bacterium to survive by destroying gingival crevice leukocytes, resulting in the suppression of local immune defences.

The interaction of LtxA with its human host is multifaceted and involves both the membrane lipids (cholesterol; Brown et al., 2013) and a cell-surface glycoprotein lymphocyte function-associated antigen 1 (LFA-1), a β_2 integrin family member (Lally et al., 1997). LtxA contains a conserved cholesterol recognition amino acid consensus motif (Brown et al., 2013; Vazquez et al., 2014) that is defined by the sequence -L/V-X_{1-5}-Y-X_{1-5}-R/K- (Epand, 2006; Li, Yao, Degenhardt, Teper, & Papadopoulos, 2001). The presence of the binding sequence (^{334}LEEYSKR^{339}) enhances the maximal affinity (minimal K_d) of the toxin for membranes containing 40% cholesterol, which is approximately four orders of magnitude (10^{-12} M) greater than the affinity for cholesterol-free membranes (10^{-8} M). LtxA associates with immune cell membranes to form round, toxin-rich patches and lipid-lined cavities that appear to be formed, as model membrane experiments suggest, through a process involving membrane bending (Brown et al., 2012). Liposomes composed of lipids that form nonlamellar phases are LtxA susceptible whereas liposomes composed of lipids that do not form nonbilayer structures are resistant to LtxA induced changes suggesting that membrane destabilisation followed by a transition from a bilayer to an inverted hexagonal phase formation of an isotropic intermediate phase lies at the heart of LtxA-mediated membrane disruption.

In addition to a direct interaction with membrane cholesterol, incubation of LtxA with detergent lysates of human immune cells in combination with immunoprecipitation with anti-LtxA antibodies (DiRienzo, Tsai, Shenker, Taichman, & Lally, 1985) resulted in the identification of two (90,000 and 165,000 kDa) cell surface glycoproteins, which also interact with the toxin (Lally et al., 1997). Trypsinization and mass spectrometric analysis of these peptides identified the smaller as β_2 and the larger as α_L, which are components of LFA-1 (Hynes, 1987), one of a family of four integrins exclusively expressed on immune cells (Gahmberg, Tolvanen, & Kotovuori, 1997; Springer, 1990; Springer, 1995). The four

integrin a subunits (α_L, α_M, α_X, and α_D) are structurally and functionally distinct from each other although all contain the β_2 subunit (Springer, 1990). LFA-1 plays a pivotal role in a number of immune cell functions (Arnaout, 1990) such leukocyte and endothelial cell interactions (Dustin & Springer, 1988), the diapedesis of cells to sites of inflammation (Ross, 1999; Springer, 1995) and the formation of the immunological synapse (Monks, Freiberg, Kupfer, Sciaky, & Kupfer, 1998). The role that β_2 integrins play in immune cell function has also led them to be used in virulence strategies of both bacteria (Hauck, Agerer, Muenzner, & Schmitter, 2006; Hauck, Borisova, & Muenzner, 2012; Pizarro-Cerda & Cossart, 2006; Relman et al., 1990; Saukkonen, Cabellos, Burroughs, Prasad, & Tuomanen, 1991; Scibelli et al., 2007; Wong & Isberg, 2005) and viruses (Hutt-Fletcher & Chesnokova, 2010; Stewart & Nemerow, 2007; Triantafilou, Takada, & Triantafilou, 2001; Wang & Springer, 1998; Wickham, Mathias, Cheresh, & Nemerow, 1993).

LFA-1 is a heterodimer made up of α_L (1145 aa) and β_2 (747 aa; Kishimoto, O'Connor, Lee, Roberts, & Springer, 1987a; Larson, Corbi, Berman, & Springer, 1989). Rotary-shadowed electron micrographs demonstrate the α_L/β_2 heterodimer elements combined at the NH_2-terminus and form a ligand-binding globular headpiece (Weisel, Nagaswami, Vilaire, & Bennett, 1992). The β_2 chain is composed of two components: (a) the ligand-binding I-like domain, (residues 104–341) and (b) the stalk (residues 1–103 that precede and residues 342–678 that follow the I-like domain; Huang, Zang, Takagi, & Springer, 2000). The two stalk components are linked by a long-range disulfide bond between Cys^3 and Cys^{425} (Calvete, Schafer, Henschen, & Gonzalez-Rodriquez, 1990). The carboxyl terminus of the stalk contains a high level of cysteine residues arranged in three or four repeating elements containing eight cysteine residues in a conserved characteristic pattern known as the cysteine-rich repeats (CRR; Kishimoto et al., 1987a; Law et al., 1987). The importance of CRR to LtxA/LFA-1 binding has been demonstrated utilising a panel of human/bovine β_2 chimeras and identifying a species-specific binding epitope located within human β_2 (Dileepan, Kachlany, Balashova, Patel, & Maheswaran, 2007). At the immune cell membrane, the heterodimer stalks separate and form individual single-pass transmembrane segments (α_L, 29 aa; β_2, 23 aa) and finally terminate in short cytosolic tails (α_L, 53 aa; β_2 46 aa), which though they lack enzymatic activity, serve as scaffolds for bidirectional signalling between the cytoplasm and extracellular ligands (Kim, Carman, & Springer, 2003).

The ability of a panel of three monoclonal anti-LFA-1 antibodies (a) TS1/18 (Sanchez-Madrid et al., 1982), (b) KIM127 (Stephens et al., 1995), and (c) KIM185 (Andrew et al., 1993) to inhibit LtxA cytolysis (Lally et al., 1997) has provided an initial indication that the contact of the toxin with LFA-1 occurs over an extensive area of the integrin. TheTS1/18 epitope, located within the ligand (I-like) domain (Huang et al., 2000), while KIM127 occurs at the second CRR (Lu, Ferzly, Takagi, & Springer, 2001; Stephens et al., 1995). Both TS1/18 and KIM127 are strong inhibitors of LFA-1-dependent adhesion. The most interesting, however, is KIM185, a mAb that effects both integrin conformational changes and ligand binding. The KIM185 epitope (residues 581–621) is located at the distal end of CRR-4 and extends onto the stalk to a point 57 amino acids from the LFA-1 transmembrane segment (Lu et al., 2001). The ability of LtxA to bind cholesterol (Brown et al., 2013; Vazquez et al., 2014), interact with extra cellular domains of LFA-1 (Lally et al., 1997), and

modify bilayer structure (Brown et al., 2012) suggests that the LtxA/LFA-1 interaction is not confined to the ectodomains of LFA-1 but rather is providing a clear pathway for LtxA to enter the cytosol.

Critical to the study of LtxA pathogenesis is an understanding the mechanism of LFA-1 and LtxA interaction, which leads to the cell death. Importantly that in addition to the LtxA ability to kill leukocytes, the toxin may exert some effects on the various LFA-1-regulated immune functions, such as activation or priming, the movement of leukocytes between blood and lymphoid tissues (Warnock, Askari, Butcher, & von Andrian, 1998), controlling cell adhesion to the extracellular matrix and immune synapse formation (Dustin et al., 1998).

Our current study, is focused on the potential interactions of LtxA with integrin cytosolic components and the cytoskeleton. Using labelled LtxA, we demonstrated that the toxin enters target cells in a LFA-1-dependent manner. We found that a translocated domain of the LtxA binds to and immobilises LFA-1 via its cytosolic domains. Florescence resonance energy transfer (FRET) microscopy indicates that internalised LtxA acts on LFA-1 from the cytosol, by not only preventing separation of the cytosolic domains upon activation but also by bringing the two domains closer together. Surface plasmon resonance (SPR) studies demonstrated LtxA affinities for the α_L and β_2 tails of LFA-1 (15 and 4.2 nM, respectively) are comparable with the affinity of talin-1 for the β_2 cytoplasmic, tail, a cytoskeletal protein (11.1 nM; Takala et al., 2008). Our results have provided new insight into the mechanism by which LtxA kills immune cells, wherein internalisation of the toxin and inhibition of integrin activation have important roles.

2 | RESULTS

2.1 | Internalisation of LtxA is dependent upon cell-surface expression of LFA-1

Fluorescent-labelled LtxA was tested for biological activity using a trypan blue exclusion test (Brogan et al., 1994). We found that our labelling protocol has no effect on the ability of LtxA labelled with DyLight™ 488 (LtxA-DY488) or LtxA labelled with fluorescein isothiocyanate (LtxA-FITC) to kill Jn.9 (Figure 1a) whereas the toxin heat inactivation prior to labelling (Δ_{HI}LtxA-DY488) abrogated its ability to kill target cells (Figure 1b). Staining of Jn.9 and its LFA-1-deficient mutant (J-β_2.7) cells with either anti-α_L (Figure 1c) or β_2 (Figure 1d) mAb and labelled LtxA demonstrate LtxA is colocalised with the α_L (Figure 1c; Pearson's coefficients for codistribution 1 = 0.75 and 2 = 0.82), as well as the β_2 (CD18) subunit of LFA-1 (Figure 1d; Pearson's coefficients for codistribution 1 = 0.65 and 2 = 0.79). In contrast, very low toxin binding was detected to the cell membranes of the LFA-1 mutant J-β_2.7 cells. Toxin binding was not observed in Jn.9 cells when target cells were incubated with Δ_{HI}LtxA. Thus, active LtxA immediately binds to the cell surface demonstrating high affinity to LFA-1-containing cell membranes. The coaggregation of LtxA and LFA-1 heterodimer components on the surface of our target cell membranes suggests that LtxA could gain access to the cytosol as individual LtxA molecules or as part of an LtxA/LFA-1 complex. Confocal microscopy (Figure 2a), flow cytometry studies (Figure 2c, and Supplementary data (Figure S1) were used to investigate this prediction.

The specificity of the LFA-1/integrin interaction was explored when LtxA-FITC was incubated with Chinese hamster ovary (CHO) cells that had been transfected and expressing $\alpha_{IIb}\beta_3$, an integrin that is not found on immune cells but is expressed on platelets and involved in their aggregation (Bennett, 2005). Confocal images of CHO cells in which the membranes were stained with WGA-AF™594 (red; Figure 2b, left panel) showed no evidence of either membrane or cytoplasmic binding after 15-min treatments with 20-nM LtxA-FITC staining while CHO/$\alpha_{IIb}\beta_3$ cells (right panel) showed evidence of membrane binding of the toxin although internalisation was not observed.

Using three Jurkat cell lines: Jn.9, LFA-1-deficient J-β_2.7 and J-β_2.7/hCD11a (Kieba et al., 2007; Weber, York, Springer, & Klickstein, 1997), LtxA-DY488 was localised by confocal fluorescence microscopy (Figure 2A) in the cytosol of the cells expressing LFA-1 (Jn.9 and J-β_2.7/hCD11a). In these cells, LtxA is found close to the plasma membrane. In contrast, J-β_2.7 cells interaction with fluorescent-labelled LtxA did not result in the toxin internalisation but the toxin was seen in clusters on the cell surface. Translocation of LtxA membrane was restored when the toxin was incubated with J-β_2.7/hCD11a cells.

Internalisation of LtxA was assessed using fluorescence quenching in combination with flow cytometry (Maldonado, Wei, Kachlany, Kazi, & Balashova, 2011; Parker, Chitcholtan, Hampton, & Keenan, 2010) in Jn.9 and J-β_2.7 cells (Figure 2C). Ten nanomolar LtxA-DY488 was incubated with cells for 15 min. Following washing (3× PBS), cell-associated fluorescence was determined by flow analysis and suggested that up to 74% of the toxin becomes cell associated within 15 min (Figure 2c, red peaks). Quenching the toxin fluorescence (trypan blue, 0.025%, 20 min) followed by scanning analysis demonstrate that while both cell lines contain membrane-associated LtxA-DY488, only LFA-1 positive (Jn.9) cells contained intracellular LtxA (Figure 2c, yellow peaks). To quench the intracellular fluorescence cells were permeabilised using 0.1% Triton X-100 for 10 min prior to 0.025% trypan blue treatment. Quenching of the fluorescence with trypan blue in permeabilised cells resulted in low cell-associated fluorescence and closely resembled untreated cells (Figure 2c, purple peaks), which served as negative controls.

2.2 | LtxA blocks LFA-1 activation

The effect of LtxA on activation of the LFA-1 heterodimer was examined using K562 cells (Lozzio & Lozzio, 1975) that had been transfected with human LFA-1 α and β genes. Two marker genes for cyan fluorescent protein (CFP) and yellow fluorescent protein (YFP) had been previously fused to the α_L and β_2 genes, respectively, prior to transfection (Kim et al., 2003). Cells were then examined by FRET microscopy following addition of either 100-nM phorbol 12-myristate 13-acetate (PMA) or 10-nM LtxA. PMA simulates LFA-1 activation and causes separation of the cytoplasmic tails and leading to a decrease in FRET efficiency (%E). The separation is transient, and %E returns to its initial value within 30 min (Figure 3a, blue bars).

In contrast, binding of LtxA to LFA-1 resulted in an increase in FRET, which is consistent with a mechanism whereby LtxA binds to and brings the cytosolic domains closer together than they are in the inactive state. Unlike PMA stimulation, this ligating effect does not appear to be transient, lasting for the duration of a 30-min experiment (Figure 3a, yellow

bars). Incubating K562 cells with LtxA for 30 min prior to the addition of 100-nM PMA abolished the cytosolic domain separation associated with PMA priming of LFA-1 (Figure 3a, green bars).

The increase in FRET we observe following LtxA treatment does not appear to be caused by LtxA-induced clustering of LFA-1. Cytochalasin D (Cyto D; 1 ng ml^{-1}), a reagent that inhibits actin polymerisation and promotes LFA-1 clustering (Yu, Wu, Gupta, & Kucik, 2010), was added to K562/α_L-CFP/β_2-YFP cells at the concentration of 1 ng ml^{-1}, and %E was measured for 30 min. No change in FRET signal was observed in these cells (Figure 3b), indicating that LFA-1 clustering is not responsible for the increase in %E we observe after treatment with LtxA but rather that it was the result of the cytoplasmic tails of LFA-1 shift closer to each other. Verification of the alteration of actin polymerisation under these conditions was performed by phalloidin staining (Chazotte, 2010). The intensity of phalloidin staining is greater in untreated cells than in Cyto D treated cells (Figure 3e), indicating that the Cyto D is inhibiting actin polymerisation.

The association of LtxA and LFA-1 in the lipid raft compartment of target cells suggests that raft integrity is critical for RTX function (Atapattu & Czuprynski, 2007; Fong et al., 2006; Martin, Uribe, Gomez-Bilbao, & Ostolaza, 2011). The role that cholesterol in LFA-1 activation was investigated by first extracting cholesterol from the K562 cells using 5-mM methyl-β-cyclodextrin (Kilsdonk et al., 1995) prior to treatment with 10-nM LtxA (Figure 3b). Cells treated with methyl-β-cyclodextrin contained $2.09 \pm 0.04 \times 10^{-7}$ μg cholesterol/cell that was statistically lower than cholesterol levels of PBS-treated control cells ($2.49 \pm 0.03 \times 10^{-7}$ μg cholesterol/cell). The extraction of cholesterol from the cells resulted in an increase in FRET to a similar extent as LtxA treatment. Addition of 10-nM LtxA for up to 30 min had no additional effect on the separation of the cytosolic domains of LFA-1 (Figure 3b).

An LtxA cytotoxicity assay (Brogan et al., 1994) verified that the FRET reagents are not toxic to K562 cells during the time scale of the experiment. LtxA, PMA, or Cyto D was added to K562 cells at the same concentrations used in the FRET experiments, and cell viability was measured for 30 min. As shown in Figure 3d, in this time, the viability of LtxA-exposed cells remained close to 100%. The viability of PMA-treated cells decreased to approximately 50%, and the viability of Cyto D exposed decreased to approximately 80%. These results indicate that most of the cells remain viable for the duration of the FRET experiment (30 min). Cell viability decreased more significantly after 1 hr of exposure to the reagents, for this reason, the FRET experiments could not be carried out to longer time points.

2.3 | LtxA binds to the cytoplasmic domains of α and β heterodimers

SPR studies demonstrating that the LtxA binds to the cytoplasmic domains of α_L and β_2 with nanomolar affinity provided a number of interesting observations (Figure 4). The short cytosolic domains of α_L (58 residues) and β_2 (46 residues) permit the synthesis of the individual peptides *in toto* (Table 1). The peptides were then coupled to Biacore™ CM5 chips, and LtxA was allowed to flow over the LFA-1-peptide chips, and the binding results were analysed by fitting to a 1:1 Langmuir binding model (Table 2). LtxA exhibits a strong

affinity for both the α_L ($K_d \approx 15$ nM) and β_2 ($K_d \approx 4.2$ nM) peptides. The association rate (k_{on}) for LtxA to the β_2 peptide (2.4×10^4 M^{-1} s^{-1}) was approximately three times higher than the association rate of LtxA binding to the α_L peptide (8.5×10^3 M^{-1} s^{-1}), whereas the dissociation rates (k_{off}) were nearly identical ($\approx 1 \times 10^{-4}$ s^{-1}). LtxA associates with the β_3 cytoplasmic tail at approximately the same rate as it does β_2 (2.6×10^4 M^{-1} s^{-1}), although the dissociation rate is considerably higher (5.9×10^{-3} s^1).

To investigate the specificity of the binding of LtxA to the LFA-1 cytosolic domains the binding to three additional integrin cytosolic domains, α_M and α_X, members of the immune cell integrin family, and β_3 were investigated. Binding of LtxA to a subunits was significantly lower (K_d for α_M = 400 nM, α_X = 180 nM) then the binding to the a_L. During our confocal microscopy studies (Figure 2c), CHO cells expressing an unrelated integrin ($\alpha_{IIb}\beta_3$) bound LtxA-FITC. We also observed that LtxA bound to the β_3 cytoplasmic domain but at a considerably lower affinity ($K_d \approx 230$ nM) than it does to β_2 thereby suggesting that there is some degree of promiscuity to the interaction.

Panels of shorter overlapping α_L and β_2 peptides (Table 1) were used to identify the region(s) that is critical for toxin binding: an N-terminal peptide, α_LN (K^{1088}-I^{1107}); an intermediate peptide, α_LI (G^{1103}-D^{1127}); and a C-terminal peptide, α_LC, (G^{1118}-D^{1145}; Table 1). LtxA bound to α_LN with the same affinity ($K_d \approx 16$ nM) as it did to full-length α_L peptide (Table 2). The association rate, k_{on}, (8.4×10^3 M^{-1} s^{-1}) and the dissociation rate, k_{off}, (1.3×10^{-4} s^{-1}) were also similar to those of LtxA binding to α_L indicating that the LtxA recognition site on the α_L tail most probably resides in the membrane proximal region of the integrin. The affinity of LtxA for the C-terminal region of α_L is considerably lower, $K_d \approx 2.9$ μM, due to the association rate (1.4×10^2 M^{-1} s^{-1}) being 20 times lower than the association rate to the full-length peptide. The dissociation rate of LtxA from α_LC was approximately equal to that of the full-length tail, 1.4×10^{-4} s^{-1}. No binding was observed when the toxin was injected over the α_LI peptide. The fact that LtxA binds both the membrane proximal and the membrane distal regions of α_L might be due to the three helix fold of the cytoplasmic tail, where Helix 1, the membrane proximal, lines up next to Helix 3, the membrane distal, a fold that is kept together by a salt bridge between K^{1117} and E^{1158} and K^{1121} and E^{1163} (Bhunia, Tang, Mohanram, Tan, & Bhattacharjya, 2009). When compared with α_L, the affinity of LtxA for the C-terminal region of α_L is considerably lower, $K_d \approx 2.9$ μM, due to the association rate (1.4×10^2 M^{-1} s^{-1}) being 20 times lower than the association rate to. The dissociation rate of LtxA from α_LC was approximately equal to that of the full-length tail, 1.4×10^{-4} s^{-1}. Only nonspecific binding of LtxA was detected when it was injected over the α_LI peptide.

Initially, an N-terminal (β_2N) and a C-terminal (β_2C) peptide was used to determine where LtxA binds to the β_2 cytoplasmic tail (Table 1), however, neither peptide bound LtxA with as high an affinity (β_2N, $K_d \approx 110$ nM; β_2C, $K_d \approx 51$ nM) as full-length β_2. The k_{on} values (6.1×10^3 M^{-1} s^{-1}) of LtxA to both peptides were four times lower than to the full-length β_2. The dissociation rates of LtxA from both β_2N1 and β_2C were greater (6.3×10^{-4} and 3.1×10^{-4} s^{-1}) than that of β_2 (1.0×10^{-4} s^{-1}). Consequently, we synthesised a second longer N-terminal peptide (β_2N2, K^{724}-N^{749}), incorporating three additional amino acid residues of the β_2 tail (WNN^{749}). The addition of these three amino acids to the peptide sequence

increased association of LtxA to the β_2N2 peptide increased the on/off rates to values that are similar to that of the full-length peptide. The dissociation rate of β_2N2 was close to the rate of β_2 peptide ($K_d \approx 9.4$ nM). The strong binding exhibited by LtxA for the region around the talin docking sequence (WNNDNPLFK^{754}) could displace talin from its cytoskeletal tether (Takala et al., 2008; Valmu, Hilden, van Willigen, & Gahmberg, 1999), a hypothesis that is consistent with our previous observations (Fong et al., 2006).

3 | DISCUSSION

LtxA structural elements suggest the toxin may be capable of interacting directly with the membrane (Fong et al., 2006; Fong et al., 2011). Model membrane studies suggest that rather than forming a protein-based structure, LtxA destabilises the membrane by inducing a transition from a bilayer to a less stable inverted hexagonal (HII) phase (Brown et al., 2012). Nonlamellar phases have been implicated in protein translocations in several systems (Ahn & Kim, 1998; Rietveld, Koorengevel, & de, 1995). In addition, some toxins may also utilise nonlamellar phases as a means to translocate the membrane (Krauss, Bond, Todd, & Wilson, 1991). The observation of LtxA-induced nonlamellar phase formation therefore suggests that LtxA toxicity may proceed through LtxA translocation through the membrane and into the cytosol. Delineation of sequela of the membrane translocation is a key issue in our understanding of the pathogenesis of this toxin.

Fluorescent-labelled LtxA was used to investigate whether the toxin is internalised in LFA-1-expressing cells. The experiment showed a clear connection between the internalisation of LtxA and the presence of LFA-1 on the cell surface (Figure 1). LtxA was internalised in both Jn.9 and J-β_2.7/CD11a cells, and interestingly, the toxin lined the inner leaflet of the membrane. J-β_2.7 cells, which do not express α_L, did not internalise LtxA, and the toxin was not observed on either the inner or outer leaflet of the membrane. Integrin heterodimers present on the cell surface seem to be important for the LtxA cell surface recognition, as seen when LtxA is introduced to cells expressing glycoprotein IIb/IIIa (integrin $\alpha_{IIb}\beta_3$), in which case the toxin was found on the cell surface but not internalised. It was possible to study internalisation using LtxA-FITC/DY488, and a cytotoxicity assay showed that the labelling had no effect on the toxin's toxicity (Figure 1b). Additionally, we therefore setup a flow cytometry experiment in which Jn.9 cells were incubated with wtLtxA and then stained with anti-LtxA to detect surface-bound and internalised LtxA. These studies showed that the LtxA internalisation is not just an artefact of fluorescent labelling but is dependent on expression of LFA-1 suggesting that it is an important part of the mechanism by which LtxA kills its host cells.

Circulating lymphocytes maintain LFA-1 and other β_2 integrins in a folded conformation with a low affinity for ligand binding. The first step in integrin activation is separation of the cytoplasmic tails. This ultrastructural change is relayed throughout the length of the heterodimer and results in unfolding of the receptor and separation of the heterodimer components. We studied the effect that the LtxA recognition and binding has on LFA-1 using K562 cells that were transfected with an $\alpha_L\beta_2$ pair whose LFA-1 cytoplasmic tails had been fused to either CFP (α_L) or YFP (β_2) (Kim et al., 2003). FRET microscopy was then used to measure the %E or average distance between the α and β heterodimer elements.

Resting cells had an average distance between α and β heterodimer elements of 7.8 nm (Figure 3a). An activation signal in the form of 100-nM PMA resulted in a decrease in %E, which is indicative of a separation of the cytoplasmic tails to 8.6 nm (Figure 3a, blue bars). The tail separation is transient, however, as %E returned to baseline value within the 30 min of the experiment. In contrast, incubation of K652 cells with 20-nM LtxA (Figure 3a, yellow bars) resulted in an increase %E, which is consistent with a decreasing distance between the α_L and β_2 heterodimer elements from 7.8 to 7.3 nm, a change that is constant for the duration of the experiment. Furthermore, once treated with LtxA, the cells no longer respond to a PMA activation indicating that the toxin is interfering with LFA-1 activation (Figure 3a, green bars).

PMA can increase intracellular Ca^{2+}levels (Xuan, Wang, & Whorton, 1992) and activate the signal transduction enzyme protein kinases C (PKC) in cells (Cullen, 2003; Niedel, Kuhn, & Vandenbark, 1983). PKC activation results in the phosphorylation of cellular proteins and modulation of multiple cellular functions (Cullen, 2003). For example, Ca^{2+}-dependent PKC, PKC-beta(I), is involved in LFA-1 activation in normal T cells. T cell locomotion is accompanied by PKC-beta-sensitive cytoskeletal rearrangements and the formation of trailing cell extensions (Volkov, Long, McGrath, Ni Eidhin, & Kelleher, 2001). Our group has previously demonstrated that LtxA causes rapid cytosolic Ca^{2+} increase, and this event is independent from toxin binding to LFA-1 (Fong et al., 2006). Therefore, we hypothesise that the effect of LtxA on LFA-1 activation is indirect and is related to the toxin induced intracellular Ca^{2+} elevation followed by activation of PKC. Among other RTX toxins, mechanistic insight into LtxA is consistent with *Bordetella pertussis* CyaA binding to the $\alpha_M\beta_2$ integrin (α_M/β_2; Osicka et al., 2015). Osicka et al. found that CyaA preferentially binds an inactive form of the integrin complement receptor 3, using a site outside of its I-domain.

Our SPR studies suggested that the LtxA recognition site on the α_L tail most probably resides in the membrane proximal region of the integrin as the N-terminal peptide (α_LN) binds LtxA with the same K_d as the entire α_L cytosolic peptide (Table 2). The cytosolic domains of β_2 integrin α-tails exhibit little homology for each other; however, all contains the GFFKR^{1094} motif (underlined; Tables 1). GFFKR^{1094}forms a salt bridge with D^{708} located on β_2 (underlined); this structure stabilises the α_L and β_2 cytoplasmic domains in a folded low-affinity state (Luo, Carman, & Springer, 2007). It is likely that the ability of LtxA to interfere with salt bridge formation impaired association with the β chain.

In addition to interfering with salt bridge formation, LtxA could block signal transduction by Rap GTPases (Kinashi, 2005), which are activated by cytosolic Ca^{2+}, diacylglycerol (Fong et al., 2006), and PMA, which we used in our current studies (Katagiri, Maeda, Shimonaka, & Kinashi, 2003; Sebzda, Bracke, Tugal, Hogg, & Cantrell, 2002; Shimonaka et al., 2003). Rap1, a small GTPase, binds to its effector molecule, regulator for cell adhesion and polarisation enriched in lymphoid tissues (RapL), the essential regulator LFA-1 activation (Katagiri et al., 2003; Shimonaka et al., 2003). The Rap1/RAPL complex then associates with the responsive site GFFKRNLKEK^{1099} (Table 1), which is located on the a heterodimer and composed of GFFKR and two adjacent lysine residues (K^{1097} and K^{1099}; Tohyama et al., 2003). Binding of the Rap1/RAPL complex to this site allows unfolding of the

heterodimer elements and subsequent ligand binding. However, our SPR experiments suggest that LtxA could block or interfere with the binding of the RAPL/Rap-1 to GFFKR. Table 2 shows that LtxA exhibits high affinity ($K_d = 1.5 \pm 0.1 \times 10^{-8}$) for this region of the α_L cytosolic domain whereas FRET microscopy (Figure 3, yellow bars) show that the cells have an elevated E% in the presence of LtxA, indicating that the αβ heterodimer components are closer together in the presence of LtxA rather than in either 100-nM PMA-treated cells or untreated controls. It is interesting to speculate on the consequences of LtxA blockage of integrin inside out signalling.

RAPL and Rap-1 have also been shown to play parts in apoptotic signalling, and similar pathways could be triggered by the interference of LFA-1 activation brought on by LtxA binding. It is unclear what the consequences of an LtxA blockage of integrin activation could be; however, both RAPL (Liu et al., 2014) and Rap-1 (Yang et al., 2013) are involved in apoptotic signalling pathways, and these could be triggered by the interference of LFA-1 activation by LtxA. Integrins also play a role in ancillary pathways involved in apoptosis (Difranco et al., 2012a), such as the Erk1/2, Akt, or JNK pathways. The interference of LtxA with LFA-1 activation response while at the same time initiating downstream integrin activation could also trigger apoptosis through a pathway such as integrin-mediated death (Krzyzowska et al., 2001; Meredith & Schwartz, 1997) or anoikis (Frisch & Screaton, 2001; Guadamillas, Cerezo, & del Pozo, 2011).

The results presented here demonstrate that T lymphocyte internalised LtxA is located at the plasma membrane and that the toxin binds α_L at its membrane-proximal region and β_2 in an intermediate region. This has led us to propose a mechanism of the LtxA/LFA-1 interaction in which LtxA binds to extracellular domains of LFA-1-initiating clustering and lipid raft formation; the toxin then transverses the cell membrane, binds the cytoplasmic tails of LFA-1, and prevents priming of the heterodimer (Figure 5). The LFA-1 α subunit contains regions that regulate the specificity of ligand-specific interactions; β subunit cytoplasmic domains are necessary and sufficient to target integrins to focal adhesions that link LFA-1 to the cytoskeleton through attachment sites that bind to various linker proteins, including α-actinin, filamin, and talin. In resting lymphocytes, β_2 integrins are constitutively linked to the actin cytoskeleton via talin, where activation of cells induces transient proteolysis and dissociation of talin, followed by reattachment of actin filaments to integrins mediated by α-actinin.

The results presented here demonstrate that internalised LtxA is located at the plasma membrane and that the toxin binds α_L at its membrane-proximal region and β_2 in an intermediate region. LtxA/LFA-1 complex was found in early endosomes of Jn.9 cells. LtxA association with LFA-1 in early endosomes (Balashova et al., submitted manuscript) suggests a receptor-mediated endocytic process of the LtxA/LFA-1 complex internalisation that may culminate in delivery of the toxin to lysosomes or the toxin release into cytosol due to LFA-1 recycling. The membrane damaging properties of LtxA are well documented (Brown et al., 2012; Lear, Furblur, Lally, & Tanaka, 1995). Although there is no direct evidence of plasma membrane damage at the LtxA internalisation step, the final target of LtxA may be an intracellular one. Such an interpretation is also consistent with recent studies that suggest lysosomal rupture as the cytotoxic mechanism (DiFranco et al., 2012b).

4 | EXPERIMENTAL PROCEDURES

4.1 | Production and purification of LtxA

A. actinomycetemcomitans strain JP2 (Tsai et al., 1979) was grown in AAGM medium (Fine et al., 1999). After bacteria were streaked on solid media, the plates were incubated at 37°C in the presence of 10% CO_2 for 2 days. Colonies were inoculated into AAGM broth and were grown for 24 hr. LtxA was purified by ammonium sulfate precipitation from the bacterial culture supernatants (Kachlany, Fine, & Figurski, 2002). The recovered precipitate was suspended in 40 ml of 10-mM KH_2PO_4, pH 6.5, and dialysed overnight. The sample was applied to a HiTRAP™ SP column (GE Healthcare™) and then eluted under isocratic conditions with 60% NaCl, 10-mM KH_2PO_4, pH 6.5. Purified protein was resolved on a 4–20% SDS-PAGE and visualized by staining with Coomassie Brilliant Blue G-250 protein stain (Bio-Rad™). Heat-inactivated LtxA (Δ_{HI}LtxA) was prepared by treatment at 65°C for 30 min. Protein concentrations were determined spectrophotometrically (NanoDrop™ 2000, Thermo Fisher™).

4.2 | Cell culture

Three Jurkat cell (Schneider, Schwenk, & Bornkamm, 1977) lines were utilised in these experiments: (a) Jn.9, a subclone of Jurkat cells; (b) J-β_2.7, a Jn.9-derived LFA-1 deletion mutant (Weber et al., 1997); and (c) J-β_2.7/hCD11a, a cell line derived from J-β_2.7 cells and transfected with α_L-containing plasmid. The cells express cell-surface LFA-1 and are susceptible to LtxA (Lally et al., 1997). The cells were maintained in RPMI 1640 medium containing 10% fetal bovine serum (FBS), 0.1-mM MEM non-essential amino acids, 1× MEM vitamin solution, and 2-mM L-glutamine, and either 0.5 μg ml^{-1} gentamicin (Jn.9 and J-β_2.7) or 200 μg/ml G418 (J-β_2.7/hCD11a) at 37°C under 5% CO_2.

K562 cells (Lozzio & Lozzio, 1975), a human erythroleukemia cell line, were transfected with α_L and β_2 heterodimers whose α_L cytoplasmic domain was fused to CFP and whose β_2 cytoplasmic domain was fused to YFP (Kim et al., 2003), respectively. These cells were provided by Dr. Timothy A. Springer, CBR, Harvard, and were maintained in RPMI 1640 medium containing 10% FBS, 100-μg ml^{-1} penicillin, 100-μg ml^{-1} streptomycin, and 0.5 mg-ml^{-1} G418.

CHO cells were obtained from ATCC, whereas Dr. Joel S. Bennett, University of Pennsylvania, provided CHO/$\alpha_{IIb}\beta_3$ cells. CHO and CHO/$\alpha_{IIb}\beta_3$ cells were propagated on glass cover slips in synthetic CD CHO medium (Life Technologies) supplemented with 50-nM hypoxanthine/8-nM thymidine and 2-mM L-glutamine. The medium for CHO/$\alpha_{IIb}\beta_3$ cells also contained Zeocin™ (0.3 mg ml^{-1}) and Geneticin™ (0.5 mg ml^{-1}).

4.3 | Cytotoxicity assay

For toxicity tests, 50-nM-purified LtxA was added to 1×10^6 Jn.9 cells and incubated for 15 hr (Brogan et al., 1994). The cell membrane permeability was determined with trypan blue assay using Vi-cell™ Cell Viability Analyzer (Beckman Coulter). Assays were performed in triplicate. Untreated cells and or cells treated with Δ_{HI}LtxA were used as controls.

4.4 | Immunofluorescence

LtxA was labelled with FITC using FITC Antibody Labeling Kit (Pierce) or DyLight™ 488 using DyLight™ Amine-Reactive dye (Pierce) according to the manufacturer's instructions. After labelling, excess of the dye was removed using a Zeba™ Spin Desalting column (40 K MWCO, Thermo Fisher™ Scientific). Cell nuclei and plasma membrane were labelled with 1-μM Hoescht 33342 and Alexa Fluor™ 594 WGA using Image iT™ LIVE Plasma Membrane and Nuclear Labeling Kit (Molecular Probes™). For LtxA and cell membrane interaction studies, 1×10^6 of Jurkat cells or CHO cells grown on cover slips were incubated with 20-nM LtxA-FITC for 15 min at 25°C. The cells were washed with PBS and fixed with 2% paraformaldehyde for 20 min, washed again, and then nuclei and plasma membrane were labelled as described above. Jurkat cells were treated with antihuman CD18 clone TS1/18 antibody (Biolegend™) (1:1,000) for 1 hr, washed, and consequently stained with donkey antimouse IgG H&L Alexa Fluor® 594 conjugated anti-body for 1 hr at 37°C. For LtxA and CD11a colocalisation studies, Jn.9 cells were treated with 20-nM LtxA-DY488 for 10 min at 37°C, were washed twice with Live cell imaging solution (Life Technologies), and incubated with antihuman CD11a Alexa Fluor™ 594 clone HI111 (Biolegend™) (1:1,000) for 1 hr at 25°C. The cell nuclei and plasma membranes were stained, washed with Live cell imaging solution, and placed in CELLview™ glass bottom dishes (Greiner Bio-One) coated with poly-L-lysine (Sigma) for imaging. For live confocal time lapse microscopy, the cell images were collected every 2–5 min for 1 hr. Colocalisation areas were determined by sorting the appropriate intersection of pixel area and intensity across each channel per Z plane with colocalised spots having a Pearson's coefficient above 0.50. Phalloidin staining was performed using F-actin Staining Kit - Green Fluorescence - Cytopainter (Abcam). The cells were examined using a Nikon A1R laser scanning confocal microscope with a 60× water objective (NA 1.2). The images were analysed using Nikon's Elements software 4.1.

4.5 | Flow cytometry

To detect surface bound LtxA, Jn.9 or J-β_2.7 cells (1×10^6 cells/run) were incubated with 20-nM LtxA-DY488 for 15 min at 37°C in PBS supplemented with 2% FBS, washed with PBS, and total cell-associated fluorescence was analysed. To quench the extracellular fluorescence, LtxA-DY488 treated cells were incubated with 0.025% trypan blue (Sigma, St. Louis, MO) for 20 min as described previously (Maldonado et al., 2011; Parker et al., 2010). To quench the intracellular fluorescence, cells were permeabilised using 0.1% Triton X-100 (Sigma, St. Louis, MO) for 10 min prior to 0.025% trypan blue treatment. Fluorescence was measured using a BD LSR II flow cytometer (BD Biosciences). In this case, ten thousand events were recorded per sample, and the mean fluorescence intensity (MFI) values were determined using WinList™7.0 software (Verity Software House). To quantitate the intracellular fluorescence, MFI values of cells pretreated with trypan blue were subtracted from the MFI values of total cell-associated LtxA-AF™488 fluorescence. No residual fluorescence was detected in 0.1% Triton X-100 permeabilised cells after the trypan blue treatment. Samples that were not treated with LtxA-DY488 served as a control.

4.6 | Peptide preparation

The peptides were generated based on the sequences corresponding to the cytosolic tails of α_L (Larson & Springer, 1990) and β_2 (Kishimoto, O'Connor, Lee, Roberts, & Springer, 1987b) LFA-1 subunits. The sequences used for the peptides design are presented in Figure S2. Peptides were procured from Peptide 2.0™ (Chantilly, VA). An N-terminal cysteine was introduced in all peptides to allow correct orientation on the sensor chip and a conservative substitution of S^{1129} for C^{1129} in α_L and α_LC peptides prevented disulfide bond-induced conformational changes and oligomerisation (Table 1).

SPR. A CM5 chip was activated with a 4-min injection of 1-ethyl-3-(3-dimethylaminopropyl) carbodiimide hydrochloride/N-hydroxysulfosuccinimide followed by a 4-min injection of 80-mM 2-(2-pyridinyldithio)-ethaneamine. Peptides (50 μg ml^{-1}) were dissolved in Hepes was then loaded on the chip. Excess 2-(2-pyridinyldithio)-ethaneamine was deactivated with a 4-min injection of 50-mM cysteine. All experiments were performed in 10-mM Hepes, 150-mM NaCl, pH 7.4. The following experimental conditions were used: 50 μl the injection sample volume; 5 min dissociation time; and 50 μl min^{-1} flow rate. The surface was regenerated with 50 μl 0.2% SDS, pH 7.5. The data were collected on a Biacore™ 3000 (GE Healthcare) and evaluated using the BIAevaluation™ software.

4.7 | FRET microscopy

K562/α_L-CFP/β_2-YFP (Aaronson et al., Kim et al., 2003) cells (1×10^6) were added to a 35-mm poly-D-lysine-coated CELLview™ tissue culture dish (Greiner Bio-One GmbH) and allowed to settle for 10 min. After several washes, the attached cells were treated with (a) 100-nM PMA (Sigma); (b) 10-nM LtxA; and (c) 10-nM LtxA for 30 min followed by 100-nM PMA or 1 ng ml^{-1} Cyto D (Sigma) treatment for 30 min at 37°C. FRET readings were collected at 5, 15, and 30 min. Stimulation of Jn.9 cells with PMA LFA-1 becomes more mobile within the lipid bilayer and clustered in rafts. To verify that none of the FRET reagents affected, K562/α_L-CFP/β_2-YFP cells viability 100-nM PMA or 1 ng ml^{-1} Cyto D were added to the cells and incubated for 30 min at 37°C, and the cytotoxicity assay was performed as described above.

CFP fluorescence intensity was measured prior to YFP bleaching, to obtain $I_{CFP\text{-}pre}$, and after bleaching, to obtain $I_{CFP\text{-}post}$. The FRET efficiency (E%) was calculated by

$$\%E = 1 - \left(I_{CFP\text{-}pre} / I_{CFP\text{-}post}\right) \quad (1)$$

The FRET efficiency was related to the distance between the tails using the relation

$$\%E = \frac{1}{1 + \left(\frac{r}{R_O}\right)^6} \quad (2)$$

where r is the distance between the two fluorophores, and R_0 is the Forster distance of CFP and YFP (5 nm). The images were captured on a Nikon™ A1R live cell confocal imaging system, and the data were analysed using Nikon™ NIS-Elements v3.2 software.

4.8 | Statistical analysis

The data were analysed using a paired Student's t test, with $p < 0.05$ considered to be statistically significant.

Supplementary Material

Refer to Web version on PubMed Central for supplementary material.

ACKNOWLEDGEMENTS

This work was supported by the United States National Institute of Health grants R01DE009517 (ETL), F32DE020950 (ACB), K99DE022795 (ACB), R01DE022465, and R01EY10420 (KBB). We thank Drs. M. Kim and T.A. Springer for supplying the K562 cells and Dr. J.S. Bennett for providing RFP-labelled CHO/$\alpha_{IIb}\beta_3$.

Funding information United States National Institute of Health, Grant/Award Numbers: R01EY10420, R01DE022465, K99DE022795, F32DE020950 and R01DE009517

REFERENCES

Ahn T, & Kim H (1998). Effects of nonlamellar-prone lipids on the ATPase activity of SecA bound to model membranes. The Journal of Biological Chemistry, 273, 21692–21698. 10.1074/jbc.273.34.21692 [PubMed: 9705304]

Andrew D, Shock A, Ball E, Ortlepp S, Bell J, & Robinson M (1993). KIM185, a monoclonal antibody to CD18 which induces a change in the conformation of CD18 and promotes both LFA-1- and CR3-dependent adhesion. European Journal of Immunology, 23, 2217–2222. 10.1002/eji.1830230925 [PubMed: 7690325]

Arnaout MA (1990). Structure and function of the leukocyte adhesion molecules CD11/CD18. Blood, 75, 1037–1050. [PubMed: 1968349]

Atapattu DN, & Czuprynski CJ (2007). Mannheimia haemolytica leukotoxin binds to lipid rafts in bovine lymphoblastoid cells and is internalized in a dynamin-2- and clathrin-dependent manner. Infection and Immunity, 75, 4719–4727. 10.1128/IAI.00534-07 [PubMed: 17682044]

Baehni P, Tsai CC, McArthur WP, Hammond BF, &Taichman NS. (1979). Interaction of inflammatory cells and oral microorganisms. VIII. Detection of leukotoxic activity of a plaque-derived gram-negative microorganism. Infection and Immunity, 24, 233–243. [PubMed: 222679]

Baehni PC, Tsai CC, McArthur WP, Hammond BF, Shenker BJ, & Taichman NS (1981). Leukotoxic activity in different strains of the bacterium Actinobacillus actinomycetemcomitans isolated from juvenile periodontitis in man. Archives of Oral Biology, 26, 671–676. 10.1016/0003-9969(81)90164-3 [PubMed: 6172101]

Bennett JS (2005). Structure and function of the platelet integrin a_{IIb}b3. The Journal of Clinical Investigation, 115, 3363–3369. 10.1172/JCI26989 [PubMed: 16322781]

Bhunia A, Tang XY, Mohanram H, Tan SM, & Bhattacharjya S (2009). NMR solution conformations and interactions of integrin aLb2 cytoplasmic tails. The Journal of Biological Chemistry, 284, 3873–3884. 10.1074/jbc.M807236200 [PubMed: 19073598]

Brogan JM, Lally ET, Poulsen K, Kilian M, & Demuth DR (1994). Regulation of Actinobacillus actinomycetemcomitans leukotoxin expression: Analysis of the promoter regions of leukotoxic and minimally leukotoxic strains. Infection and Immunity, 62, 501–508. [PubMed: 8300209]

Brown AC, Balashova NV, Epand RM, Epand RF, Bragin A, Kachlany SC, … Lally ET (2013). Aggregatibacter actinomycetemcomitans leukotoxin utilizes a cholesterol recognition/amino acid

consensus site for membrane association. The Journal of Biological Chemistry, 288, 23607–23621. 10.1074/jbc.M113.486654 [PubMed: 23792963]

Brown AC, Boesze-Battaglia K, Du Y, Stefano FP, Kieba IR, Epand RF, … Lally ET (2012). Aggregatibacter actinomycetemcomitans leukotoxin cytotoxicity occurs through bilayer destabilization. Cellular Microbiology, 14, 869–881. 10.1111/j.1462-5822.2012.01762.x [PubMed: 22309134]

Calvete JJ, Schafer W, Henschen A, & Gonzalez-Rodriquez J (1990). C-terminal amino acid determination of the transmembrane subunits of the human platelet fibrinogen receptor, the GPIIb/IIIa complex. FEBS Letters, 263, 43–46. 10.1016/0014-5793(90)80701-J [PubMed: 2332052]

Chazotte B (2010). Labeling cytoskeletal F-actin with rhodamine phalloidin or fluorescein phalloidin for imaging. Cold Spring Harbor Protocols, 2010. pdb prot4947

Cullen PJ (2003). Calcium signalling: The ups and downs of protein kinase C. Current Biology, 13, R699–R701. 10.1016/j.cub.2003.08.041 [PubMed: 13678606]

DiFranco KM, Gupta A, Galusha LE, Perez J, Nguyen TV, Fineza CD, & Kachlany SC (2012b). Leukotoxin (Leukothera(R)) targets active leukocyte function antigen-1 (LFA-1) protein and triggers a lysosomal mediated cell death pathway. The Journal of Biological Chemistry, 287, 17618–17627. 10.1074/jbc.M111.314674 [PubMed: 22467872]

Difranco KM, Gupta A, Galusha LE, Perez J, Nguyen T-V, Fineza CD, & Kachlany SC (2012a). Leukotoxin (Leukothera®) targets active leukocyte function antigen-1 (LFA-1) protein and triggers a lysosomal mediated cell death pathway. Journal of Biological Chemistry, 287, 17618–17627. 10.1074/jbc.M111.314674 [PubMed: 22467872]

DiFranco KM, Kaswala RH, Patel C, Kasinathan C, & Kachlany SC (2013). Leukotoxin kills rodent WBC by targeting leukocyte function associated antigen 1. Comparative Medicine, 63, 331–337. [PubMed: 24209968]

Dileepan T, Kachlany SC, Balashova NV, Patel J, & Maheswaran SK (2007). Human CD18 is the functional receptor for Aggregatibacter actinomycetemcomitans leukotoxin. Infection and Immunity, 75, 4851–4856. 10.1128/IAI.00314-07 [PubMed: 17635865]

DiRienzo JM, Tsai CC, Shenker BJ, Taichman NS, & Lally ET (1985). Monoclonal antibodies to leukotoxin of Actinobacillus actinomycetemcomitans. Infection and Immunity, 47, 31–36. [PubMed: 3965404]

Dustin ML, Olszowy MW, Holdorf AD, Li J, Bromley S, Desai N, ... Shaw AS(1998). A novel adaptor protein orchestrates receptor patterning and cytoskeletal polarity in T-cell contacts. Cell, 94, 667–677. 10.1016/S0092-8674(00)81608-6 [PubMed: 9741631]

Dustin ML, S Springer TA (1988). Lymphocyte function-associated antigen-1 (LFA-1) interaction with intercellular adhesion molecule-1 (ICAM-1) is one of at least three mechanisms for lymphocyte adhesion to cultured endothelial cells. The Journal of Cell Biology, 107, 321–331. 10.1083/jcb.107.1.321 [PubMed: 3134364]

Epand RM (2006). Cholesterol and the interaction of proteins with membrane domains. Progress in Lipid Research, 45, 279–294. 10.1016/j.plipres.2006.02.001 [PubMed: 16574236]

Fine DH, Furgang D, Schreiner HC, Goncharoff P, Charlesworth J, Ghazwan G, … Figurski DH (1999). Phenotypic variation in Actinobacillus actinomycetemcomitans during laboratory growth: Implications for virulence. Microbiology, 145(Pt 6), 1335–1347. 10.1099/13500872-145-6-1335 [PubMed: 10411260]

Fong KP, Pacheco CM, Otis LL, Baranwal S, Kieba IR, Harrison G, ... Lally ET. (2006). Actinobacillus actinomycetemcomitans leukotoxin requires lipid microdomains for target cell cytotoxicity. Cellular Microbiology, 8, 1753–1767. 10.1111/j.1462-5822.2006.00746.x [PubMed: 16827908]

Fong KP, Tang HY, Brown AC, Kieba IR, Speicher DW, Boesze-Battaglia K, S Lally ET (2011). Aggregatibacter actinomycetemcomitans leukotoxin is post-translationally modified by addition of either saturated or hydroxylated fatty acyl chains. Molecular Oral Microbiology, 26, 262–276. 10.1111/j.2041-1014.2011.00617.x [PubMed: 21729247]

Frisch SM, S Screaton RA (2001). Anoikis mechanisms. Current Opinion in Cell Biology, 13, 555–562. 10.1016/S0955-0674(00)00251-9 [PubMed: 11544023]

Gahmberg CG, Tolvanen M, S Kotovuori P (1997). Leukocyte adhesion: Structure and function of human leukocyte b2-integrins and their cellular ligands. European Journal of Biochemistry, 245, 215–232. 10.1111/j.1432-1033.1997.00215.x [PubMed: 9151947]

Guadamillas MC, Cerezo A, S del Pozo MA (2011). Overcoming anoikis: Pathways to anchorage-independent growth in cancer. Journal of Cell Science, 124, 3189–3197. 10.1242/jcs.072165 [PubMed: 21940791]

Haubek D, S Johansson A (2014). Pathogenicity of the highly leukotoxic JP2 clone of Aggregatibacter actinomycetemcomitans and its geographic dissemination and role in aggressive periodontitis. Journal of Oral Microbiology, 6 10.3402/jom.v6.23980

Hauck CR, Agerer F, Muenzner P, S Schmitter T (2006). Cellular adhesion molecules as targets for bacterial infection. European Journal of Cell Biology, 85, 235–242. 10.1016/j.ejcb.2005.08.002 [PubMed: 16546567]

Hauck CR, Borisova M, S Muenzner P (2012). Exploitation of integrin function by pathogenic microbes. Current Opinion in Cell Biology, 24, 637–644. 10.1016/j.ceb.2012.07.004 [PubMed: 22884865]

Hoglund Aberg C, Haubek D, Kwamin F, Johansson A, S Claesson R (2014). Leukotoxic activity of Aggregatibacter actinomycetemcomitans and periodontal attachment loss. PLoS One, 9, e104095. 10.1371/journal.pone.0104095

Huang C, Zang Q, Takagi J, S Springer TA (2000). Structural and functional studies with antibodies to the integrin b2 subunit. A model for the I-like domain. The Journal of biological chemistry, 275, 21514–21524. 10.1074/jbc.M002286200 [PubMed: 10779511]

Hutt-Fletcher LM, S Chesnokova LS (2010). Integrins as triggers of Epstein-Barr virus fusion and epithelial cell infection. Virulence, 1, 395–398. 10.4161/viru.1.5.12546 [PubMed: 21178476]

Hynes RO (1987). Integrins: A family of cell surface receptors. Cell, 48, 549–554. 10.1016/0092-8674(87)90233-9 [PubMed: 3028640]

Kachlany SC, Fine DH, S Figurski DH (2002). Purification of secreted leukotoxin (LtxA) from Actinobacillus actinomycetemcomitans. Protein Expression and Purification, 25, 465–471. 10.1016/S1046-5928(02)00037-2 [PubMed: 12182827]

Kachlany SC, Schwartz AB, Balashova NV, Hioe CE, Tuen M, Le A, … Rao J (2010). Anti-leukemia activity of a bacterial toxin with natural specificity for LFA-1 on white blood cells. Leukemia Research, 34, 777–785. 10.1016/j.leukres.2009.08.022 [PubMed: 19747730]

Katagiri K, Maeda A, Shimonaka M, & Kinashi T (2003). RAPL, a Rap1-binding molecule that mediates Rapl-induced adhesion through spatial regulation of LFA-1. Nature Immunology, 4, 741–748. 10.1038/ni950 [PubMed: 12845325]

Kieba IR, Fong KP, Tang HY, Hoffman KE, Speicher DW, Klickstein LB, & Lally ET (2007). Aggregatibacter actinomycetemcomitans leukotoxin requires b sheets 1 and 2 of the human CDlla b-propeller for cytotoxicity. Cellular Microbiology, 9, 2689–2699. 10.1111/j.1462-5822.2007.00989.x [PubMed: 17587330]

Kilsdonk EP, Yancey PG, Stoudt GW, Bangerter FW, Johnson WJ, Phillips MC, & Rothblat GH (1995). Cellular cholesterol efflux mediated by cyclodextrins. The Journal of Biological Chemistry, 270, 17250–17256. 10.1074/jbc.270.29.17250 [PubMed: 7615524]

Kim M, Carman CV, & Springer TA (2003). Bidirectional transmembrane signaling by cytoplasmic domain separation in integrins. Science, 301, 1720–1725. 10.1126/science.1084174 [PubMed: 14500982]

Kinashi T (2005). Intracellular signalling controlling integrin activation in lymphocytes. Nature Reviews. Immunology, 5, 546–559. 10.1038/nri1646

Kishimoto TK, O'Connor K, Lee A, Roberts TM, & Springer TA (1987a). Cloning of the b subunit of the leukocyte adhesion proteins: homology to an extracellular matrix receptor defines a novel supergene family. Cell, 48, 681–690. 10.1016/0092-8674(87)90246-7 [PubMed: 3028646]

Kishimoto TK, O'Connor K, Lee A, Roberts TM, & Springer TA (1987b). Cloning of the beta subunit of the leukocyte adhesion proteins: Homology to an extracellular matrix receptor defines a novel supergene family. Cell, 48, 681–690. 10.1016/0092-8674(87)90246-7 [PubMed: 3028646]

Krauss JC, Bond LM, Todd RF,. I.I.I., & Wilson JM(1991). Expression of retroviral transduced human CD18 in murine cells: An in vitro model of gene therapy for leukocyte adhesion deficiency. Human Gene Therapy, 2, 221–228. 10.1089/hum.1991.2.3-221 [PubMed: 1684295]

Krzyzowska M, Sabri F, De MA, Missailidis C, Schollenberger A, Niemialtowski MG, & Chiodi F (2001). Cross-linking of LFA-1 molecule enhances Fas mediated apoptosis of Jurkat and Burkitt lymphoma cell lines. Cell Death and Differentiation, 8, 1123–1124. 10.1038/sj.cdd.4400927 [PubMed: 11687890]

Lally ET, Kieba IR, Sato A, Green CL, Rosenbloom J, Korostoff J, ... Billings PC(1997). RTX toxins recognize a b2 integrin on the surface of human target cells. The Journal of Biological Chemistry, 272, 30463–30469. 10.1074/jbc.272.48.30463 [PubMed: 9374538]

Larson RS, Corbi AL, Berman L, & Springer T (1989). Primary structure of the leukocyte function-associated molecule-1 a subunit: An integrin with an embedded domain defining a protein superfamily. The Journal of Cell Biology, 108, 703–712. 10.1083/jcb.108.2.703 [PubMed: 2537322]

Larson RS, & Springer TA (1990). Structure and function of leukocyte integrins. Immunological Reviews, 114, 181–217. 10.1111/j.1600-065X.1990.tb00565.x [PubMed: 2196220]

Law SK, Gagnon J, Hildreth JE, Wells CE, Willis AC, & Wong AJ (1987). The primary structure of the b-subunit of the cell surface adhesion glycoproteins LFA-1, CR3 and p150,95 and its relationship to the fibronectin receptor. The EMBO Journal, 6, 915–919. 10.1002/j.1460-2075.1987.tb04838.x [PubMed: 2954816]

Lear JD, Furblur UG, Lally ET, & Tanaka JC (1995). Actinobacillus actinomycetemcomitans leukotoxin forms large conductance, voltage-gated ion channels when incorporated into planar lipid bilayers. Biochimica et Biophysica Acta, 1238, 34–41. 10.1016/0005-2736(95)00086-I [PubMed: 7544624]

Li H, Yao Z, Degenhardt B, Teper G, & Papadopoulos V (2001). Cholesterol binding at the cholesterol recognition/interaction amino acid consensus (CRAC) of the peripheral-type benzodiazepine receptor and inhibition of steroidogenesis by an HIV TAT-CRAC peptide. Proceedings of the National Academy of Sciences of the United States of America, 98, 1267–1272. 10.1073/pnas.98.3.1267 [PubMed: 11158628]

Liu G, Shi Z, Jiao S, Zhang Z, Wang W, Chen C, … Zhang M (2014). Structure of MST2 SARAH domain provides insights into its interaction with RAPL. Journal of Structural Biology, 185, 366–374. 10.1016/j.jsb.2014.01.008 [PubMed: 24468289]

Lozzio CB, & Lozzio BB (1975). Human chronic myelogenous leukemia cell-line with positive Philadelphia chromosome. Blood, 45, 321–334. [PubMed: 163658]

Lu C, Ferzly M, Takagi J, & Springer TA (2001). Epitope mapping of antibodies to the C-terminal region of the integrin b 2 subunit reveals regions that become exposed upon receptor activation. Journal of Immunology, 166, 5629–5637. 10.4049/jimmunol.166.9.5629

Luo BH, Carman CV, & Springer TA (2007). Structural basis of integrin regulation and signaling. Annual Review of Immunology, 25, 619–647. 10.1146/annurev.immunol.25.022106.141618

Maldonado R, Wei R, Kachlany SC, Kazi M, & Balashova NV (2011). Cytotoxic effects of Kingella kingae outer membrane vesicles on human cells. Microbial Pathogenesis, 51, 22–30. 10.1016/j.micpath.2011.03.005 [PubMed: 21443941]

Martin C, Uribe KB, Gomez-Bilbao G, & Ostolaza H (2011). Adenylate cyclase toxin promotes internalisation of integrins and raft components and decreases macrophage adhesion capacity. PLoS One, 6, e17383. 10.1371/journal.pone.0017383

Meredith JE Jr., & Schwartz MA (1997). Integrins, adhesion and apoptosis. Trends in Cell Biology, 7, 146–150. 10.1016/S0962-8924(97)01002-7 [PubMed: 17708932]

Monks CR, Freiberg BA, Kupfer H, Sciaky N, & Kupfer A (1998). Three-dimensional segregation of supramolecular activation clusters inT cells. Nature, 395, 82–86. 10.1038/25764 [PubMed: 9738502]

Niedel JE, Kuhn LJ, & Vandenbark GR (1983). Phorbol diester receptor copurifies with protein kinase C. Proceedings of the National Academy of Sciences of the United States of America, 80, 36–40. 10.1073/pnas.80.1.36 [PubMed: 6296873]

Osicka R, Osickova A, Hasan S, Bumba L, Cerny J, & Sebo P (2015). Bordetella adenylate cyclase toxin is a unique ligand of the integrin complement receptor 3. eLife, 4, e10766. 10.7554/eLife.10766

Parker H, Chitcholtan K, Hampton MB, & Keenan JI (2010). Uptake of Helicobacter pylori outer membrane vesicles by gastric epithelial cells. Infection and Immunity, 78, 5054–5061. 10.1128/IAI.00299-10 [PubMed: 20876296]

Pizarro-Cerda J, & Cossart P (2006). Bacterial adhesion and entry into host cells. Cell, 124, 715–727. https://doi.org/10.1016Z.cell.2006.02.012 [PubMed: 16497583]

Relman D, Tuomanen E, Falkow S, Golenbock DT, Saukkonen K, & Wright SD (1990). Recognition of a bacterial adhesion by an integrin: Macrophage CR3 (aMb2, CD11b/CD18) binds filamentous hemagglutinin of Bordetella pertussis. Cell, 61, 1375–1382. 10.1016/0092-8674(90)90701-F [PubMed: 2364431]

Rietveld AG, Koorengevel MC, & de KB (1995). Non-bilayer lipids are required for efficient protein transport across the plasma membrane of Escherichia coli. The EMBO Journal, 14, 5506–5513. 10.1002/j.1460-2075.1995.tb00237.x [PubMed: 8521807]

Ross R (1999). Atherosclerosis: An inflammatory disease. The New England Journal of Medicine, 340, 115–126. 10.1056/NEJM199901143400207 [PubMed: 9887164]

Sanchez-Madrid F, Krensky AM, Ware CF, Robbins E, Strominger JL, Burakoff SJ, & Springer TA (1982). Three distinct antigens associated with human T-lymphocyte-mediated cytolysis: LFA-1, LFA-2, and LFA-3. Proceedings of the National Academy of Sciences of the United States of America, 79, 7489–7493. 10.1073/pnas.79.23.7489 [PubMed: 6984191]

Saukkonen K, Cabellos C, Burroughs M, Prasad S, & Tuomanen E (1991). Integrin-mediated localization of Bordetella pertussis within macrophages: Role in pulmonary colonization. The Journal of Experimental Medicine, 173, 1143–1149. 10.1084/jem.173.5.1143 [PubMed: 2022924]

Schneider U, Schwenk HU, & Bornkamm G (1977). Characterization of EBV-genome negative “null” and “T” cell lines derived from children with acute lymphoblastic leukemia and leukemic transformed non-Hodgkin lymphoma. International Journal of Cancer, 19, 621–626. 10.1002/ijc.2910190505 [PubMed: 68013]

Scibelli A, Roperto S, Manna L, Pavone LM, Tafuri S, Della MR, & Staiano N (2007). Engagement of integrins as a cellular route of invasion by bacterial pathogens. Veterinary Journal, 173, 482–491. 10.1016/j.tvjl.2006.01.010

Sebzda E, Bracke M, Tugal T, Hogg N, & Cantrell DA (2002). Rap1A positively regulates T cells via integrin activation rather than inhibiting lymphocyte signaling. Nature Immunology, 3, 251–258. 10.1038/ni765 [PubMed: 11836528]

Shahabuddin N, Boesze-Battaglia K, & Lally ET (2016). Trends in susceptibility to aggressive periodontal disease. Int J Dent Oral Health, 2. 10.16966/2378-7090.197

Shimonaka M, Katagiri K, Nakayama T, Fujita N, Tsuruo T, Yoshie O, & Kinashi T (2003). Rap1 translates chemokine signals to integrin activation, cell polarization, and motility across vascular endothelium under flow. The Journal of Cell Biology, 161, 417–427. 10.1083/jcb.200301133 [PubMed: 12707305]

Springer TA (1990). Adhesion receptors of the immune system. Nature, 346, 425–434. 10.1038/346425a0 [PubMed: 1974032]

Springer TA (1995). Traffic signals on endothelium for lymphocyte recirculation and leukocyte emigration. Annual Review of Physiology, 57, 827–872. 10.1146/annurev.ph.57.030195.004143

Stephens P, Romer JT, Spitali M, Shock A, Ortlepp S, Figdor CG, & Robinson MK (1995). KIM127, an antibody that promotes adhesion, maps to a region of CD18 that includes cysteine-rich repeats. Cell Adhesion and Communication, 3, 375–384. 10.3109/15419069509081292 [PubMed: 8640375]

Stewart PL, & Nemerow GR (2007). Cell integrins: Commonly used receptors for diverse viral pathogens. Trends in Microbiology, 15, 500–507. https://doi.org/10.1016Z.tim.2007.10.001 [PubMed: 17988871]

Taichman NS, Simpson DL, Sakurada S, Cranfield M, DiRienzo J, & Slots J (1987). Comparative studies on the biology of Actinobacillus actinomycetemcomitans leukotoxin in primates. Oral

Microbiology and Immunology, 2, 97–104. 10.1111/jM399-302X.1987.tb00270.x [PubMed: 3507626]

Takala H, Nurminen E, Nurmi SM, Aatonen M, Strandin T, Takatalo M, … Fagerholm SC (2008). b2 integrin phosphorylation onThr^{758} acts as a molecular switch to regulate 14–3-3 and filamin binding. Blood, 112, 1853–1862. 10.1182/blood-2007-12-127795 [PubMed: 18550856]

Tohyama Y, Katagiri K, Pardi R, Lu C, Springer TA, & Kinashi T (2003). The critical cytoplasmic regions of the a_L/β_2 integrin in Rap1-induced adhesion and migration. Molecular Biology of the Cell, 14, 2570–2582. 10.1091/mbc.e02-09-0615 [PubMed: 12808052]

Triantafilou K, Takada Y, & Triantafilou M (2001). Mechanisms of integrin-mediated virus attachment and internalization process. Critical Reviews in Immunology, 21, 311–322. [PubMed: 11922076]

Tsai CC, McArthur WP, Baehni PC, Hammond BF, &Taichman NS (1979). Extraction and partial characterization of a leukotoxin from a plaque-derived Gram-negative microorganism. Infection and Immunity, 25, 427–439. [PubMed: 113347]

Valmu L, Hilden TJ, van Willigen G, & Gahmberg CG (1999). Characterization of b2 (CD18) integrin phosphorylation in phorbol ester-activated T lymphocytes. The Biochemical Journal, 339(Pt 1), 119–125. 10.1042/bj3390119 [PubMed: 10085235]

Vazquez RF, Maté SM, Bakás LS, Fernández MM, Malchiodi EL, & Herlax VS (2014). Novel evidence for the specific interaction between cholesterol and a-haemolysin of Escherichia coli. Biochemical Journal, 458, 481–489. 10.1042/BJ20131432 [PubMed: 24351077]

Volkov Y, Long A, McGrath S, Ni Eidhin D, & Kelleher D (2001). Crucial importance of PKC-beta(I) in LFA-1-mediated locomotion of activated T cells. Nature Immunology, 2, 508–514. 10.1038/88700 [PubMed: 11376337]

Wang J, & Springer TA (1998). Structural specializations of immunoglobulin superfamily members for adhesion to integrins and viruses. Immunological Reviews, 163, 197–215. 10.1111/j.1600-065X.1998.tb01198.x [PubMed: 9700512]

Warnock RA, Askari S, Butcher EC, & von Andrian UH (1998). Molecular mechanisms of lymphocyte homing to peripheral lymph nodes. The Journal of Experimental Medicine, 187, 205–216. 10.1084/jem.187.2.205 [PubMed: 9432978]

Weber KS, York MR, Springer TA, & Klickstein LB (1997). Characterization of lymphocyte function-associated antigen 1 (LFA-1)-deficientT cell lines: The aL and b2 subunits are interdependent for cell surface expression. Journal of Immunology, 158, 273–279.

Weisel JW, Nagaswami C, Vilaire G, & Bennett JS (1992). Examination of the platelet membrane glycoprotein IIb-IIIa complex and its interaction with fibrinogen and other ligands by electron microscopy. The Journal of Biological Chemistry, 267, 16637–16643. [PubMed: 1644841]

Welch RA (1991). Pore-forming cytolysins of gram-negative bacteria. Molecular Microbiology, 5, 521–528. 10.1111/j.1365-2958.1991.tb00723.x [PubMed: 2046545]

Wickham TJ, Mathias P, Cheresh DA, & Nemerow GR (1993). Integrins a_vb_3 and a_vb_5 promote adenovirus internalization but not virus attachment. Cell, 73, 309–319. 10.1016/0092-8674(93)90231-E [PubMed: 8477447]

Wong KW, & Isberg RR (2005). Emerging views on integrin signaling via Rac1 during invasin-promoted bacterial uptake. Current Opinion in Microbiology, 8, 4–9. 10.1016/j.mib.2004.12.009 [PubMed: 15694850]

Xuan YT, Wang OL, & Whorton AR (1992). Role of protein kinase C (PKC) in mediating Ca2+ entry in vascular smooth muscle cells. Advances in Experimental Medicine and Biology, 311, 427–428. 10.1007/978-1-4615-3362-7_65 [PubMed: 1529782]

Yang B, Sun H, Li W, Zhu C, Jian B, Hou W, … Yao B (2013). Expression of Rap1 during germ cell development in the rat and its functional implications in 2-methoxyacetic acid-induced spermatocyte apoptosis. Urology, 81, 696–698.

Yu T, Wu X, Gupta KB, & Kucik DF (2010). Affinity, lateral mobility, and clustering contribute independently to b2-integrin-mediated adhesion. American Journal of Physiology. Cell Physiology, 299, C399–C410. 10.1152/ajpcell.00039.2009 [PubMed: 20445173]

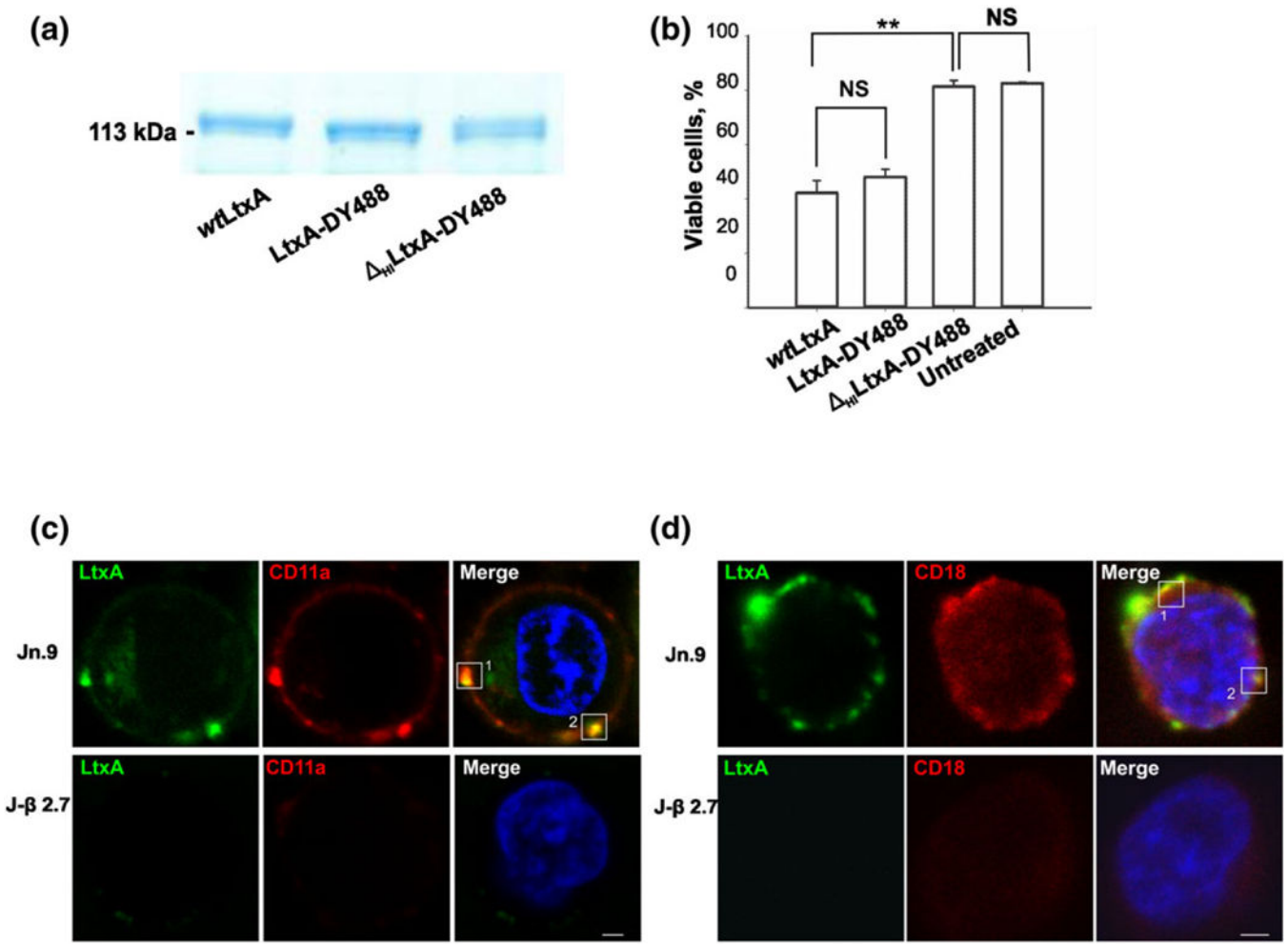

FIGURE 1.

Membrane colocalisation of LtxA in LFA-1 positive and LFA-1 negative cells. (a) The SDS-PAGE of *wt*LtxA, LtxA-DY488, and Δ_{HI}LtxA-DY488 samples, (5 μg/well loaded). (b) Trypan blue assay (Brogan et al., 1994) demonstrating cytotoxicity of *wt*LtxA, LtxA-DY488, and A_{HI}LtxA-DY488 on Jn.9 cells (15 hr, 50 nM of the toxins added). (c,d) Confocal images of Jn.9 and J-β_2.7 cells showing colocalisation of LtxA and α_L subunit after the treatment with 20-nM LtxA-DY488 (green) for 10 min at 37°C and anti-α_L antibody conjugated with Alexa Fluor™594 (red) (c). Confocal images of Jn.9 and J-β_2.7 cells showing colocalisation of LtxA and β_2 subunit after the treatment with LtxA-DY488 (green) and antihuman CD18 clone TS1/18 antibody (Biolegend™), which were recognised with donkey antimouse IgG H&L Alexa Fluor® 594 conjugated antibody (red) (d). Cell nuclei were stained with Hoechst 33342 (blue). Insets demonstrate the areas of colocalisation on the plasma membrane: α_L (Pearson's coefficients for codistribution 1 = 0.75 and 2 = 0.82) and β_2 (Pearson's coefficients for codistribution 1 = 0.65 and 2 = 0.79). Representative images are shown. Scale bars = 5 μm. LtxA: leukotoxin; LFA-1: lymphocyte function-associated antigen 1

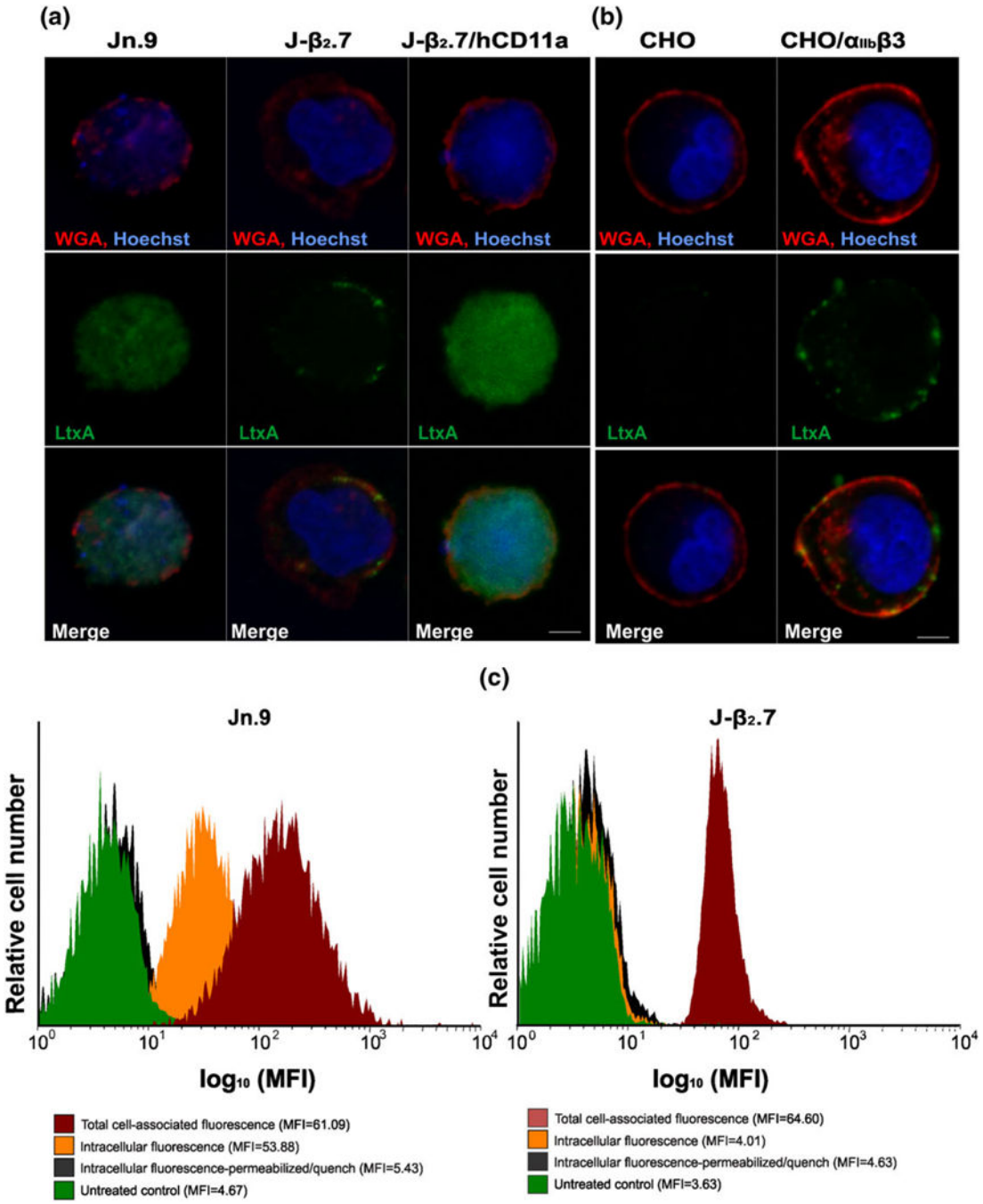

FIGURE 2.

Internalisation of LtxA in LFA-1-positive and LFA-1-negative cells. (a) Confocal images of Jn.9, J-β_2-7, and J-β_2.7/hCD11a cells after 15 min treatments with 20-nM LtxA-DY488 (green). Cell nuclei were stained with Hoechst 33342 (blue), and membranes were stained with WGA-AF™ 594 (red). Left panel shows that LtxA internalised by cells naturally (Jn.9) or heterologously (J-β_2.7/hCD11a) expressing human α_L, which was evident from the intense green fluorescence found in cell membranes and cytosols. In contrast, J-β_2.7 cells, which do not express human α_L, the toxin accumulated on the membrane surface and did

not internalise. (b) CHO and CHO/$\alpha_{IIb}\beta_3$ cells (CHO cells expressed RFP-tagged $\alpha_{IIb}\beta_3$) were incubated with 20-nM LtxA-DY488. LtxA-DY488 (green) was found on the CHO/$\alpha_{IIb}\beta 3$ cell surface but was not internalised. Representative images are shown. Scale bars = 5 μm. (c) Flow cytometry analysis was used to detect LtxA in LFA-1 positive (Jn.9) or LFA-1-negative mutant cells (J-β_2.7). Cells (1×10^6 cells) were incubated with 20-nM LtxA-DY488 (20 min) and then were analysed by flow cytometry, and the total cell-associated fluorescence was determined (a) (red peak). The extracellular fluorescence of the cells was quenched (0.025% trypan blue; Maldonado et al., 2011; Parker et al., 2010). Intracellular fluorescence cells were determined by permeabilizing the cells (0.1% Triton X-100) for 10 min prior to 0.025% trypan blue treatment. Intracellular fluorescence was again measured by flow analysis as described above. Ten thousand events were recorded per sample, and the mean fluorescence intensity (MFI) values were determined again using WinList™ software. To quantitate the intracellular fluorescence, MFI values of cells pretreated with trypan blue were subtracted from the MFI values of total cell-associated LtxA-DY488 fluorescence. No residual fluorescence was detected in 0.1% Triton X-100 permeabilised cells after the trypan blue treatment. Permeabilised LtxA-DY488 cells (black) resulted in low cell-associated fluorescence and closely resembled untreated cells (green) served as a negative control. The data shown are representative of three independent experiments. LtxA: leukotoxin; CHO: Chinese hamster ovary; LFA-1: lymphocyte function-associated antigen 1

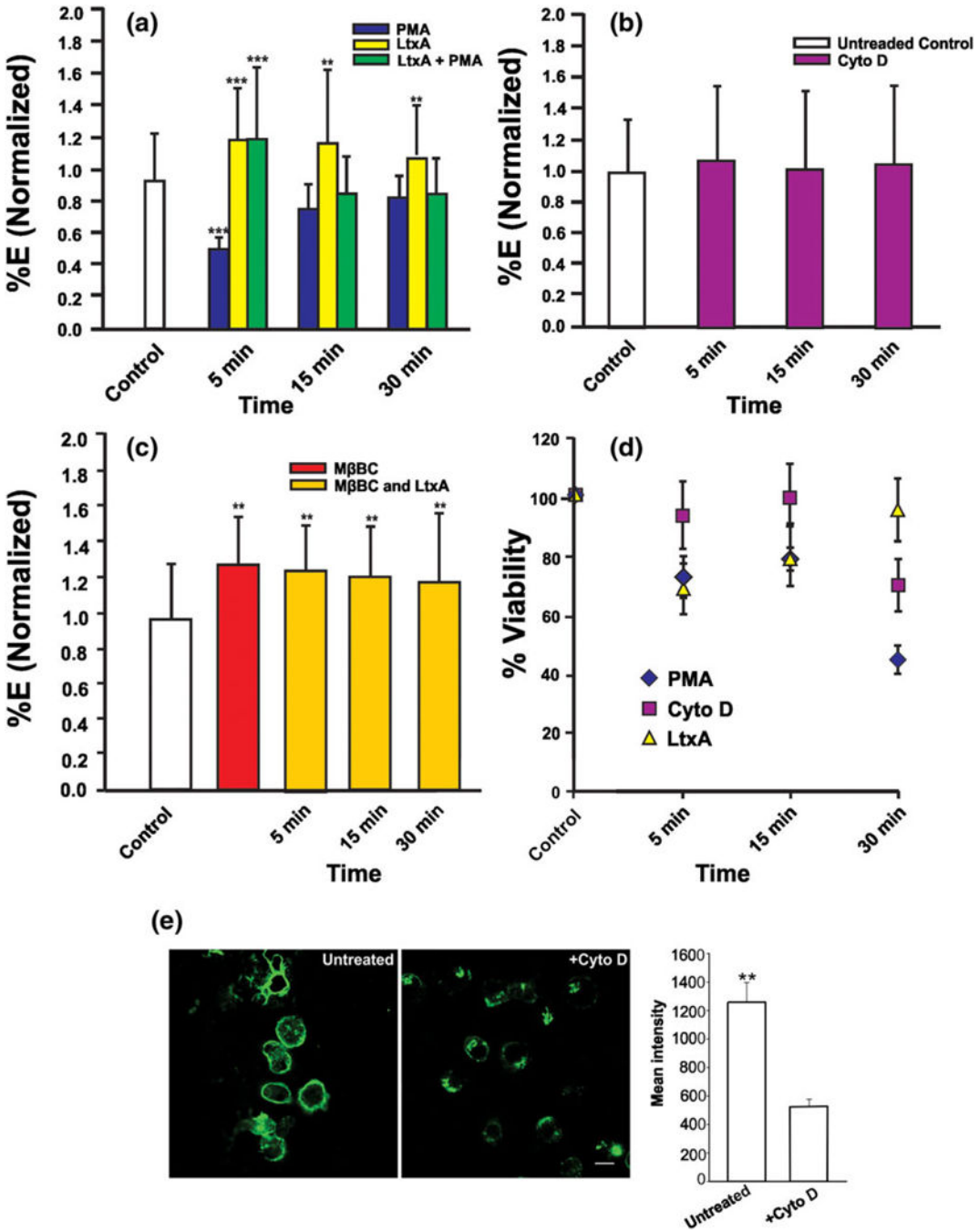

FIGURE 3.

FRET analysis of LFA-1 and LtxA interaction. (a) LFA-1 priming with 100-nM PMA (blue bars, $n = 4–9$ cells) initially separated the α and β cytosolic domains, resulting in a reduction in FRET relative to untreated cells (white bar, $n = 87$ cells). Addition of LtxA led to an increase in FRET throughout the duration of the experiment (yellow bars, $n = 27–48$ cells). Preincubation of cells with LtxA for 30 min ablated the ability of PMA to induce domain separation, as evidenced by the constant FRET signal for the duration of the experiment (green bars, $n = 11–14$ cells). (b) Treatment of cells with 1 ng ml^{-1} Cyto D, which inhibits

actin polymerisation and promotes LFA-1 clustering, had no effect on the FRET signal (n = 14–23 cells). (c) The extraction of cholesterol from the K562 cell membranes using mβCD prior to treatment with 10-nM LtxA resulted in an increase in FRET to an extent that is similar to LtxA treatment. The addition of 10-nM LtxA for up to 30 min (yellow bars) had no additional effect on the separation of the cytosolic domains of LFA-1. (d) The viability of the K562 cells when treated with the FRET reagents, PMA (blue diamonds), Cyto D (red squares), and LtxA (green triangles) was followed over 1 hr. *** $p < 0.001$, ** $p < 0.005$, * $p < 0.01$, n = 4–87 cells. Bars show SEM. (e) Confocal images of green fluorescent phalloidin conjugate staining (green) in untreated cells and in Cyto D treated cells. Representative images are shown. Scale bars = 5 μm. Average green fluorescence intensity per cell (n = 50) is shown on the right. Bars indicate SEM. ** $p < 0.005$. LtxA: leukotoxin; PMA: phorbol 12-myristate 13-acetate; Cyto D: Cytochalasin D; LFA-1: lymphocyte function-associated antigen 1

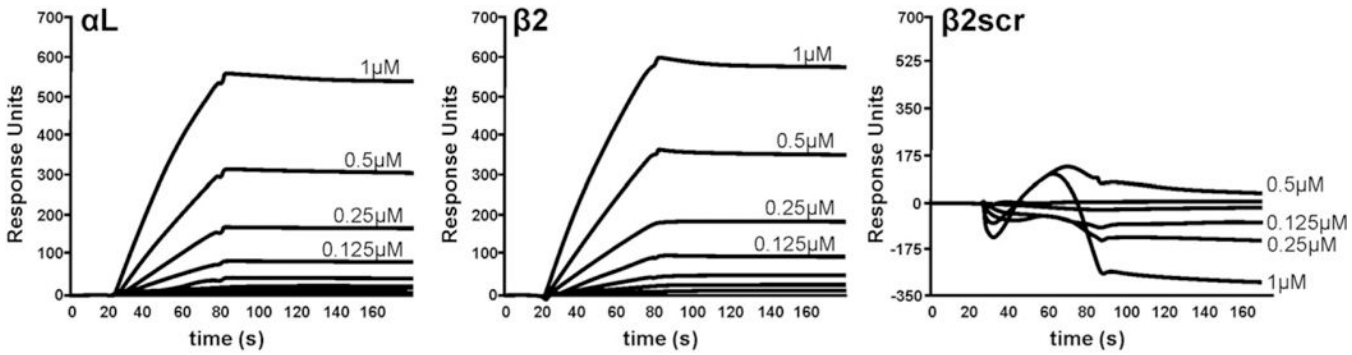

FIGURE 4.

Sensorgrams showing the association and dissociation of leukotoxin to the α_L, β_2, and β_2*scr* cytoplasmic tails. Injections were made as 2× dilution series from 1 to 0.002 μM, as marked. Sequences of the peptides used in the SPR experiments are provided in Table 1. Each sensorgram represents a typical scan

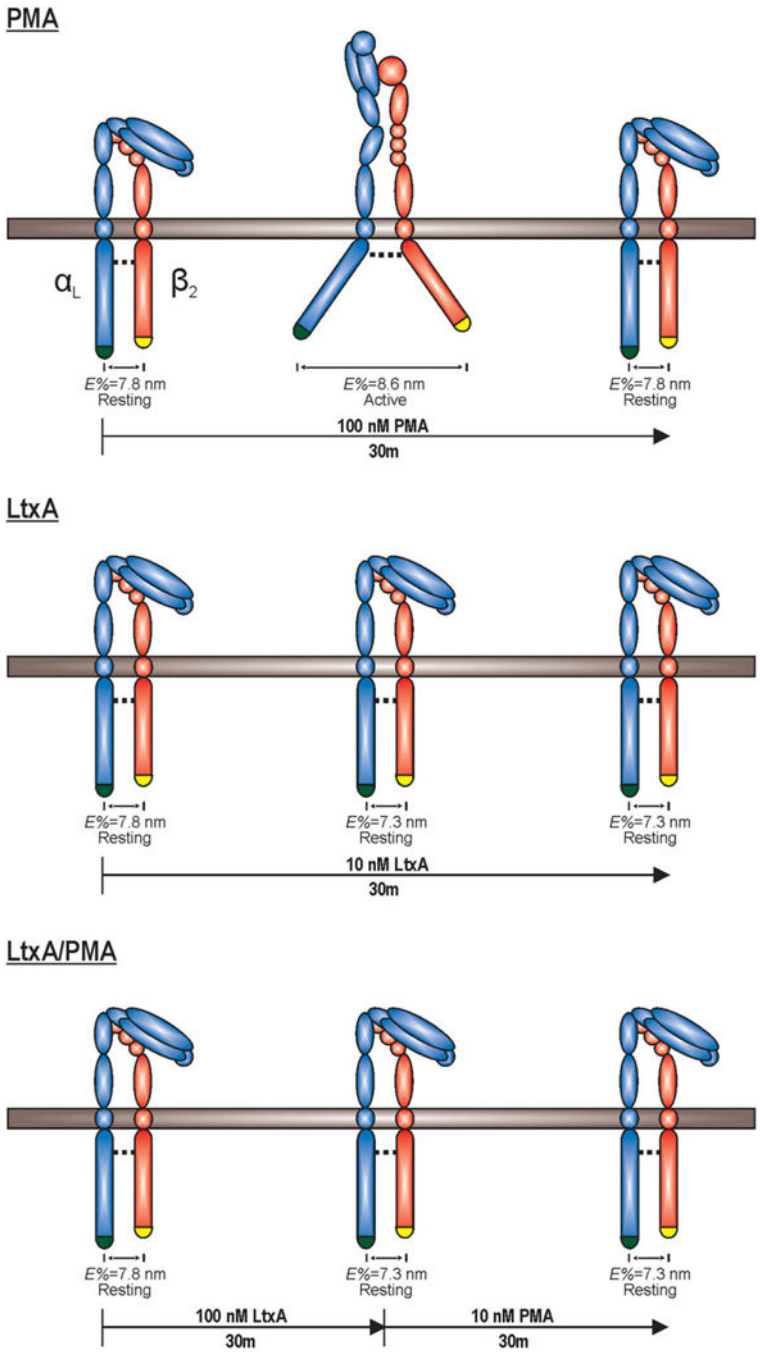

FIGURE 5.

LtxA binds to the cytoplasmic domains of α and β subunits. K562 cells were transfected with α_L and β_2 heterodimers whose cytoplasmic domain had been fused to either CFP (α_L) or YFP (β_2), respectively. The cells were then examined by FRET microscopy following addition of either 100-nM PMA or 10-nM LtxA. PMA causes separation of the cytoplasmic tails and a decrease FRET efficiency (%E) simulating LFA-1 activation. In contrast, incubation of cells with LtxA resulted in an increase in FRET, which is consistent with bringing the cytosolic domains closer together than they are in the inactive state. Unlike

PMA stimulation, this ligating effect does not appear to be transient. Incubating K562 cells with LtxA for 30 min prior to the addition of 100-nM PMA abolished the cytosolic domain separation associated with PMA priming of LFA-1. LtxA: leukotoxin; PMA: phorbol 12-myristate 13-acetate; LFA-1: lymphocyte function-associated antigen 1

TABLE 1

Peptides used in the SPR experiments [a]

αL	
α_L	KVGFFKRNLKEKMEAGRGVPNGIPAEDSEQ LASGQEAGDPGSLKPLHEKDSESGGGKD[1145]
α_LN	KVGFFKRNLKEKMEAGRGVPNGI[1107]
α_LI	GRGVPNGIPAEDSEQLASGQEAGDP[1127]
α_LC	GQEAGDPGSLKPLHEKDSESGGGKD[1145]
α_M	
α_M	KLGFFKRQYKDMMSEGGSPGAEPQ[1136]
α_X	
α_X	KVGFFKRQYKEMM EEANGQIAPE NGTQTPSPPSEK1144
β_2	
β_2	KALIHLSDLREYRRFEKEKLKSQWNN DNPLFKSATTTVM NPKFAES[747]
β_2N	KALIHLSDLREYRRFEKEKLKSQ[724]
β_2N2	KALIHLSDLREYRRFEKEKLKSQWNN[727]
β_2C	LKSQWNNDNPLFKSATTTVMNPKFAES[747]
β_2*scr*	PKFQIAESDLHDLKLLYRNKALTVMN KESNFKSATWNKSRETPRFE
β_3	
β_3	KLLITIHDRKEFAKFEEERARAKWDTA NNPLYKEATSTFTNITYRGT[762]
β_3*scr*	PHGEAITYRTEFKNRTDIARKWADTFA ETLNKTIETKNLAKLESRYF

Note. An N-terminal cysteine was added to all peptides to facilitate attachment and orientation to the Biacore™ CM5 sensor chip. A conservative substitution of S^{1129} for C^{1129} on α_L α_LC and α_LI peptides was necessary to prevent disulfide bond-induced conformational changes and oligomerisation; *scr* are scrambled α and β peptides. SPR: surface plasmon resonance

[a]Data are taken from UniProt (http://www.uniprot.org). Amino acid numbering does not include the signal sequence.

TABLE 2

Kinetic constants of the binding of LtxA to cytosolic α_L, α_M, α_X, β_2, and β_3, as well as to the truncation peptides α_LN, α_LI, α_LC, β_2N1, β_2N2, and β_2C and scrambled (β_2*scr* and β_3*scr*)

Peptide	k_{on} (M^{-1} s^{-1})	K_{off} (s^{-1})	K_a (M^{-1})	K_d(M)
α_L	8.5 (±1.0) × 10^3	1.2 (±0.2) × 10^{-4}	6.9 (±0.5) × 10^7	1.5 (±0.1) × 10^{-8}
α_LN	8.4 (±1.4) × 10^3	1.3 (±0.2) × 10^{-4}	6.6 (±0.3) × 10^7	1.6 (±0.1) × 10^{-8}
α_LI	No binding detected			
α_LC	4.7 (±0.7) × 10^2	1.4 (±0.7) × 10^{-4}	3.7 (±0.4) × 10^5	2.9 (±0.5) × 10^{-6}
α_M	2.8 (±0.6) × 10^4	1.1 (±0.2) × 10^{-2}	2.5 (±0.1) × 10^6	4.0 (±0.1) × 10^{-7}
α_X	1.3 (±0.5) × 10^5	2.2 (±0.4) × 10^{-2}	5.7 (±1.6) × 10^6	1.8 (±0.3) × 10^{-7}
β_2	2.4 (±0.3) × 10^4	1.0 (±0.3) × 10^{-4}	2.4 (±0.3) × 10^8	4.2 (±0.3) × 10^{-9}
β2N	6.1 (±0.5) × 10^3	6.3 (±0.7) × 10^{-4}	9.6 (±0.3) × 10^6	1.1 (±0.1) × 10^{-7}
β_2N2	1.4 (±0.2) × 10^4	1.3 (±0.1) × 10^{-4}	1.1 (±0.1) × 10^8	9.4 (±0.9) × 10^{-9}
β_2C	6.1 (±0.8) × 10^3	3.1 (±0.4) × 10^{-4}	2.0 (±0.3) × 10^7	5.1 (±0.8) × 10^{-8}
β_2*scr*	No binding detected			
β_3	2.6 (±0.5)×10^4	5.9 (±0.3) × 10^{-3}	4.4(±0.5) × 10^6	2.3(±0.3) × 10^{-7}
β_3*scr*	No binding detected			

Note. All kinetic constants were calculated using the BIAevaluation™ software, using a 1:1 Langmuir model. The kinetic constants represent the average of three separate experiments ± the standard deviation.